(Received 15 October 2025, Accepted 24 November 2025, Scheduled 11 December 2025)

A Flexible Hexagonal Loop Monopole Antenna with Embedded EBG for SAR Reduction in WBAN

Shital B. Gundre* and Varsha R. Ratnaparkhe

ENTC Department, Government College of Engineering Aurangabad, Chatrapati Sambhajinagar, India

ABSTRACT: This paper introduces a novel compact, flexible hexagonal loop shaped patch antenna embedded with a novel electromagnetic bandgap (EBG) structure. The proposed antenna with EBG is designed for ISM band operation, targeting 2.45 GHz wearable applications in close proximity to the human body. The EBG unit cell is formed using a rectangular patch which has nested U shaped slots with a stretched strip of inverted U shaped slot at bottom. Both hexagonal loop antenna and 2×2 EBG array were simulated using Ansys HFSS (High Frequency Structure Simulator). A key aim of this research is to achieve specific absorption rate (SAR) reduction. The effectiveness of the EBG array structure in reducing surface waves and dropping down the SAR is demonstrated using a multilayer human tissue equivalent phantom comprising skin, fat, muscle, and bone layers. It confirms that the obtained SAR values are within the safety limits set by regulatory authorities. The simulation results are verified and validated by the measurements of fabricated antenna. Furthermore, the antenna was experimentally assessed in terms of its performance under bending and in practical on-body conditions.

1. INTRODUCTION

Wireless Body Area Networks (WBANs) reinforce continuous health monitoring and athletic performance analytics, which has intensified research on wearable antenna. These antennae must operate reliably in close proximity to lossy, high-permittivity human tissue and remain functional under daily motion and deformation [1]. Consequently, the demand for flexible, body-worn patch antennas continues to grow. Such antennas are required to maintain stable performance under mechanically and electromechanically harsh conditions, while also offering flexibility [2], and a low profile, compact design [3]. It must have broadband impedance matching to mitigate detuning and low specific absorption rate to satisfy safety and market requirements [4]. To adopt a wearable antenna on different body parts, the flexible textile dielectrics such as jeans, cotton, felt, and flexible polymer composites are used for both radiators like EBG and patch antennas as a substrate because they enable conformal, low mass, and bend-tolerant implementations without catastrophic detuning and facilitating integration into garments for wearable applications. When these antennas are used close to the human body, some of the electromagnetic energy is absorbed by body tissue. This absorption is measured by specific absorption rate (SAR) which is an important safety factor, as high SAR values can pose potential health risks. SAR quantifies how much radio frequency (RF) energy is absorbed by human tissue per unit mass, serving as a key metric for the evaluation of RF exposure in body-worn wireless devices. This study follows IEEE C95.1 standards and Federal Communications Commission (FCC) guidelines. The FCC's SAR limit for localized exposure over 1 g of tissue is 1.6 W/kg and International Commission on Non-Ionizing Radiation Protection (ICNIRP) standard allows over 10 g of tissue 2 W/kg; both are widely used benchmarks in wearable and body-centric antenna studies [5–7].

Researchers have proposed several strategies to reduce SAR in wearable antennas. One common approach is the use of engineered surfaces like electromagnetic band gap structures, artificial magnetic conductors, and high-impedance surfaces (HISs), which act as reflective layers behind the antenna. These structures help supress surface wave propagation and redirect radiation away from the body [8]. Uniplanar (via-less) EBGs are especially attractive for garments because they are textile friendly, preserve softness, reduce mass, and simplify fabrication while maintaning the in-phase reflection band near the Industrial, Scientific, and Medical (ISM) frequencies used by wireless body area networks (WBANs) [9].

In past, various types of EBG structures were reported by different authors for single and dual band. In [10], a Yagi-Uda antenna operating at 2.4 GHz is designed with a flexible polyester sheet as a substrate. To make it suitable for body worn communication, it is backed with a square via-type EBG (particle swarm optimization (PSO) optimized unit cell) as a 3×3 array, which helps to suppress electromagnetic (EM) wave propagation and achieves SAR value as 0.07 W/kg, indicating excellent SAR reduction. Directional gain is also improved from 3.41 to 8.53 dBi. While achieving this the bandwidth shrinks from 345 MHz to 33 MHz. In [11], the authors report a monopole antenna made up by using paper as a substrate and ring-shaped EBG (inkjet printed) as a 4×3 array. However, the gain of antenna is reduced from 9 to 0.95 dBi which indicates very low gain, indicating suitability for short range links. In [12], a fork shape EBG is integrated with a wearable antenna as a 2×1 array of EBG and achieves SAR as 0.695 W/kg. Here, limited

* Corresponding author: Shital B. Gundre (sbg_etx@geca.ac.in).

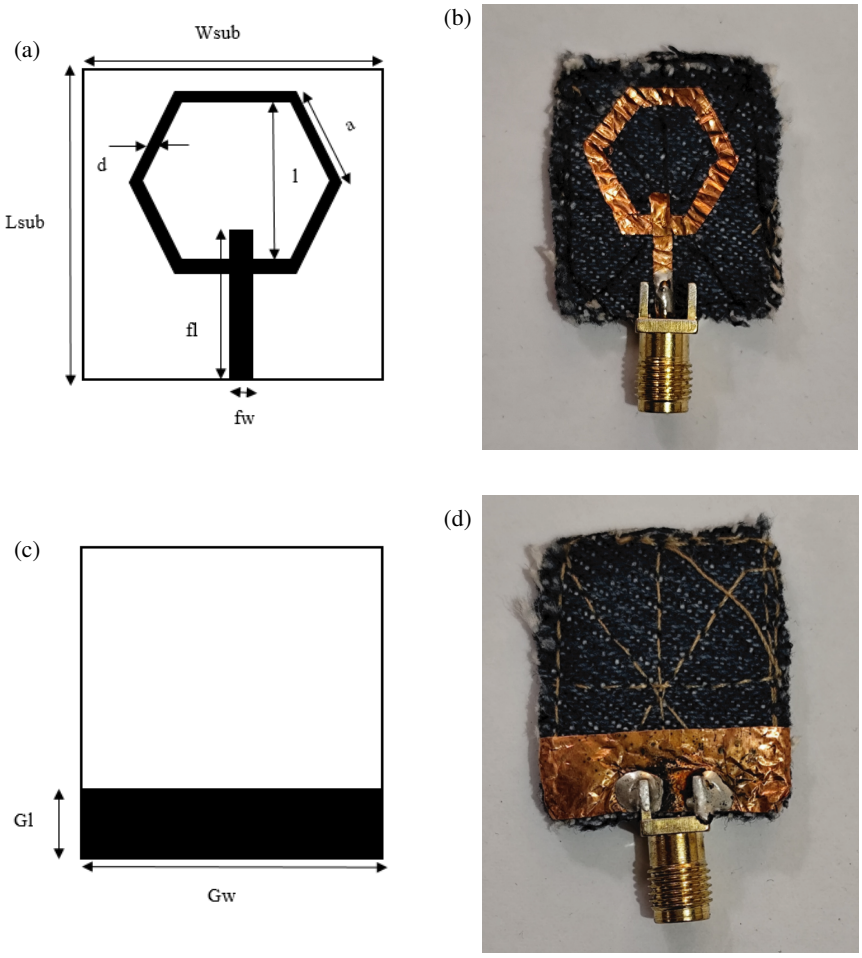

FIGURE 1. Hexagonal loop antenna configuration. (a) Hexagonal loop antenna top view. (b) Fabricated hexagonal loop antenna top view. (c) Hexagonal loop antenna bottom view. (d) Fabricated hexagonal loop antenna bottom view.

array size shrinks the back radiation suppression, and the rigid substrate RO4003 is unsuitable for wearable applications. Ref. [13] reports a dual-band 2.4 GHz fractal antenna backed by a 3×3 array of square EBG cells (50 mm $\times$ 50 mm per unit) to catch SAR reduction as 0.024 W/kg with excellent flexibility. In [14], the authors describe a circular ring slot patch integrated with a 3×3 rectangular EBG array measuring 81 mm $\times$ 81 mm $\times$ 4 mm presented alongside equivalent circuit model, and the authors assert that the designed low SAR makes it suitable for wearable use. However, the bending analysis is not provided to prove the structure suitability for body worn applications. In [15], a compact wearable textile antenna, measuring 46 mm $\times$ 46 mm, is fabricated on a flexible jeans substrate, embedded with a 2×2 EBG array, and designed for medical applications (2.4 GHz) reported to give higher gain with reduced SAR. Although these designs give promising electromagnetic performance, their increased thickness limits their feasibility in wearable Medical Body Area Network (MBAN) platforms. In [16], the authors report that an antenna having printed M-shaped operating at 2.45 GHz is paired with Jerusalem Cross artificial magnetic conductor, and the pairing of the JC AMC mitigates electromagnetic interference. Here, achieved gain and bandwidth are limited. The authors describe a textile dual band antenna covering 2.4 GHz and 5 GHz integrated with 4×4 EBG lattice having dimensions as $100 \times 100 \times 4.5\,\text{mm}^3$, achieving strong front to back ratio (FBR) and low SAR across a broad operating in [17]. In [18], antenna integrated with an EBG structure made of double concentric square shapes is presented. These EBG unit cells support dual band operation at 2.4 GHz and 5 GHz with overall dimensions of $120 \times 120 \times 4.3\,\text{mm}^3$. The study scrutinizes a reduction in radiation penetrating into the human body. The EBG proved is large in size with limited bending tests.

In the view of identified challenges and performance constraints, this study proposes a hexagonal loop antenna with an EBG designed for ISM band applications at 2.45 GHz. The proposed antenna with an EBG array has a compact size as $47 \times 43 \times 3\,\text{mm}^3$. The main aim of the antenna embedded with an EBG array is to reduce SAR level by suppressing back radiations. Section 2 describes the design of flexible hexagonal loop antenna and EBG. Section 3 details the antenna embedded with EBG array and study of water and sweat absorption on antenna performance. Section 4 focuses on bending effect on antenna embedded with EBG. Section 5 describes the SAR analysis, and Section 6 gives the conclusion.

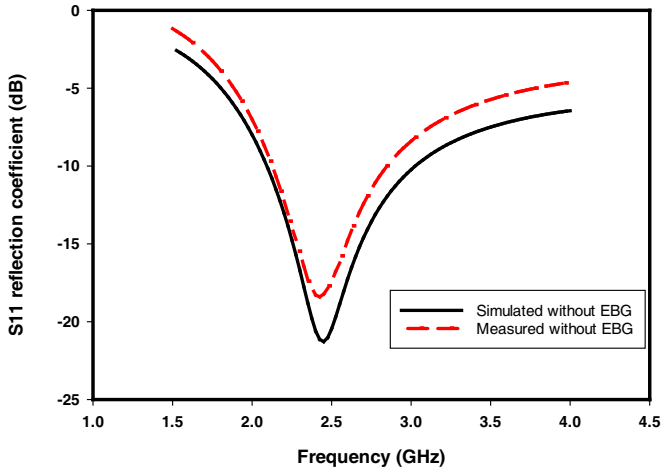

FIGURE 2. Simulated and measured reflection coefficient (S_{11}) comparison of proposed antenna.

2. FLEXIBLE MONOPOLE ANTENNA AND EBG DESIGN

2.1. Flexible Hexagonal Loop Antenna Design

The proposed novel flexible hexagonal loop monopole wearable antenna is conceived and optimized for operation at 2.45 GHz using (Ansys HFSS) a finite-element full wave solver, emphasizing compact integration, mechanical compliance, and textile compatibility. The radiating patch of proposed antenna adopts a hexagonal loop geometry formed by six equal straight copper tape segments (thickness 0.17 mm, conductivity 5.8×107 S/m) enabling a short conformal current path with controllable input impedance while preserving structural simplicity suitable for bending on fabric substrates. The proposed antenna is realized on a jeans fabric substrate selected for robustness and comfort in wearable contexts. The textile exhibits a relative permittivity of 1.78 with loss tangent of 0.085 at the design frequency, and a thickness of 0.8 mm, having size $L_{sub} = 27$ mm and $W_{sub} = 21$ mm [19]. A 50 Ω microstrip feed is used for compact, ground-referenced integration, feed length $f_l = 12.2$ mm, feed width $f_w = 2$ mm. The hexagonal loop geometry is defined by side length $a = 8$ mm, conductor strip width $d = 1$ mm, and overall loop span $l = 16$ mm. These values yield an effective resonant path length near a quarter wavelength when being combined with fringing fields and proximity to the partial ground plane, centering the response within the 2.45 GHz ISM band. The ground plane is implemented on the reverse side as partial ground with a width $G_w = 21$ mm and length $G_l = 5.7$ mm. This partial ground height and width are chosen to stabilize the input impedance and radiation characteristics while preserving the compact form factor and facilitating forward-directed radiation away from the body. The final prototype was fabricated as per the above specifications with top (heaxagonal loop and microstrip feed with the jeans fabric as the dielectric) and bottom (partial ground) views confirming a thin conformal layout suited for wearable assembly. Figure 1 depicts the proposed antenna prototype, with annotated geometry shown in top and bottom views.

Figure 2 shows both the simulated and measured S_{11} results for the designed antenna. In the simulation, the antenna without EBG structure resonates at 2.45 GHz, where it has an S_{11} value of -21 dB which indicates a strong impedance match and efficient radiation at that frequency. On the other hand, the measured results from the fabricated prototype, shown in Figure 3, exhibit a resonance at 2.42 GHz with an S_{11} of -18.5 dB. Although a small frequency shift is observed between the simulated and measured responses, the overall agreement remains strong. This close correlation validates the accuracy of the simulation models and confirms the effectiveness of the proposed antenna design.

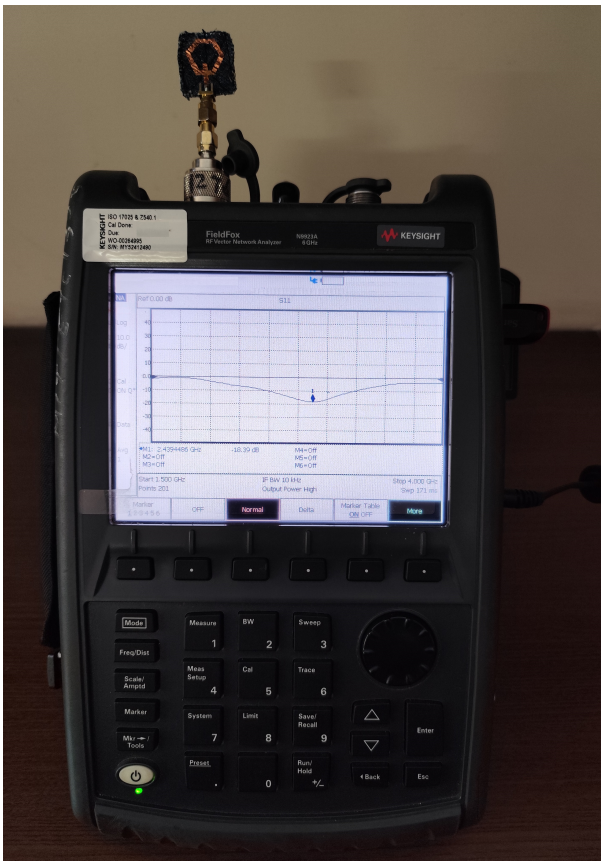

FIGURE 3. VNA measurement of fabricated hexagonal loop antenna.

2.2. Proposed EBG Design

The proposed electromagnetic bandgap (EBG) unit cell is formed using a rectangular patch which has nested U-shaped slots with a stretched strip of inverted U shaped slot at bottom. The geometry incorporates a stretched strip with inverted U shaped slot which is embedded into adjacent EBG cell to enhance inter cell coupling. The EBG unit cell is implemented on the same jeans textile substrate as the antenna to ensure material consistency and predictable EM behaviour across the stack. The novelty of the design resides in the reconfigured nested U structure coupling mechanism, which effectively alters the surface current distribution and modifies the equivalent LC resonance characteristics. This EBG unit cell topology is adopted to realize a 0° reflection phase crossing at the

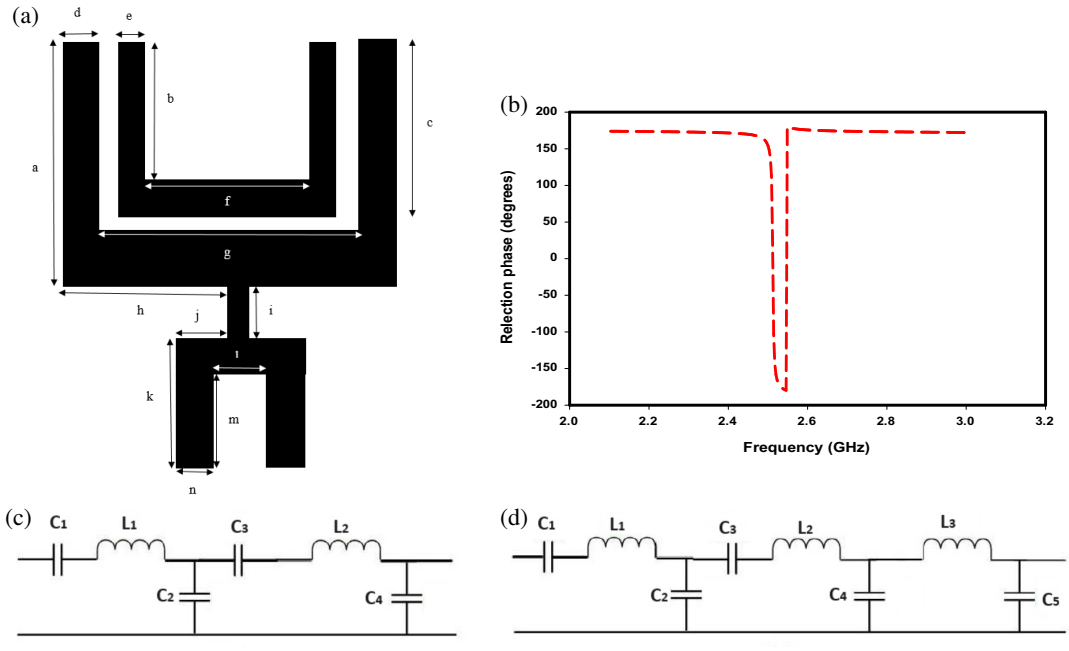

FIGURE 4. Proposed EBG. (a) EBG unit cell. (b) Phase response. (c) Equivalent circuit of EBG unit cell in X-direction. (d) Equivalent circuit of EBG unit cell Y-direction.

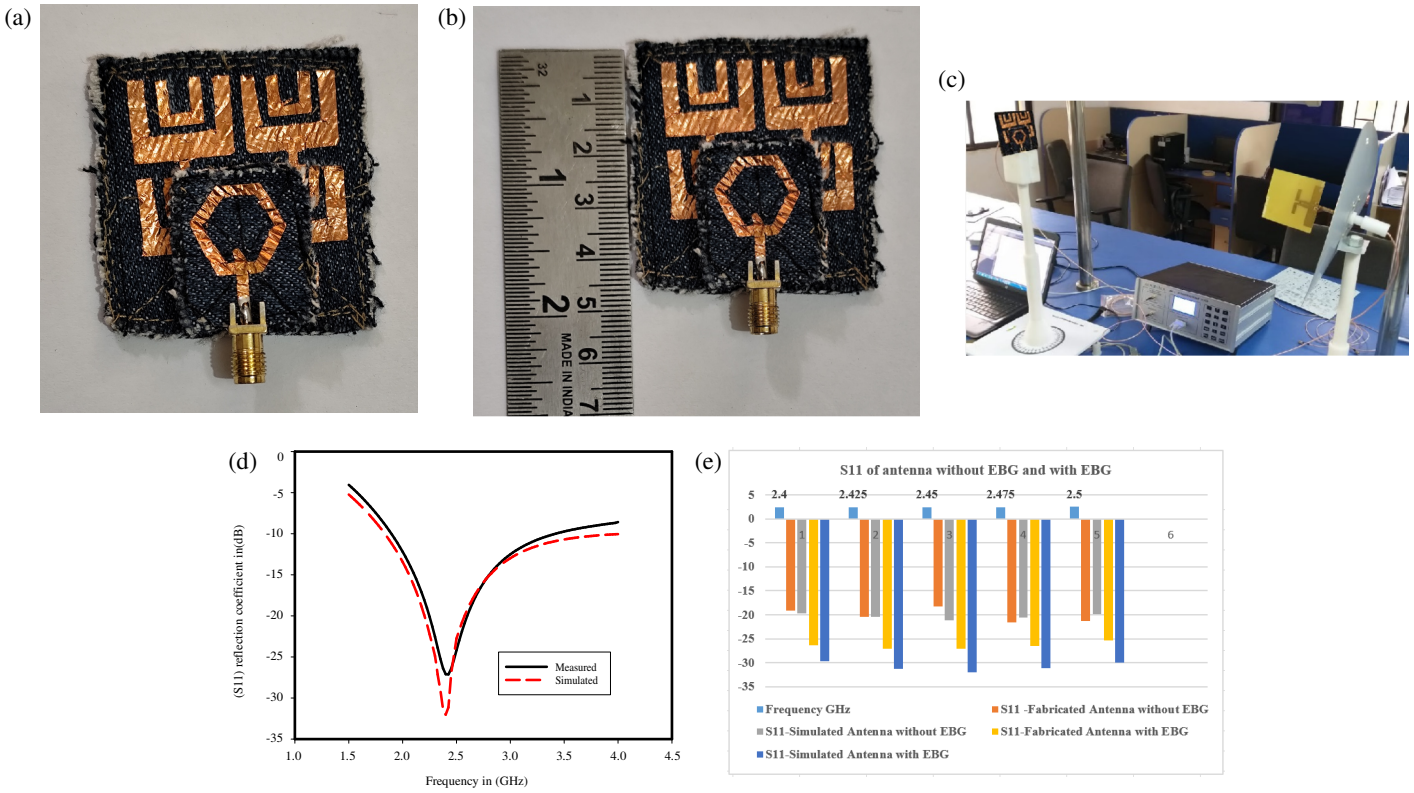

FIGURE 5. (a) Antenna embedded with EBG array. (b) Size of fabricated atenna embedded with EBG array. (c) Measurement setup. (d) S_{11} of antenna with EBG simulation and measurement comparison. (e) Comparison of simulated and measured results of antenna without EBG and with EBG.

operating frequency. The phase behaviour of the reflection coefficient is evaluated by analysing the EBG unit cell using master-slave boundary conditions along the lateral sides and wave port excitation applied at the top interface. Under this configuration, the proposed EBG structure exhibits a zero degree reflection phase at the resonating frequency 2.5 GHz as illustrated in Figure 4(b). This characteristic confirms the EBG ability to mimic the behaviour of an artificial magnetic conduc-

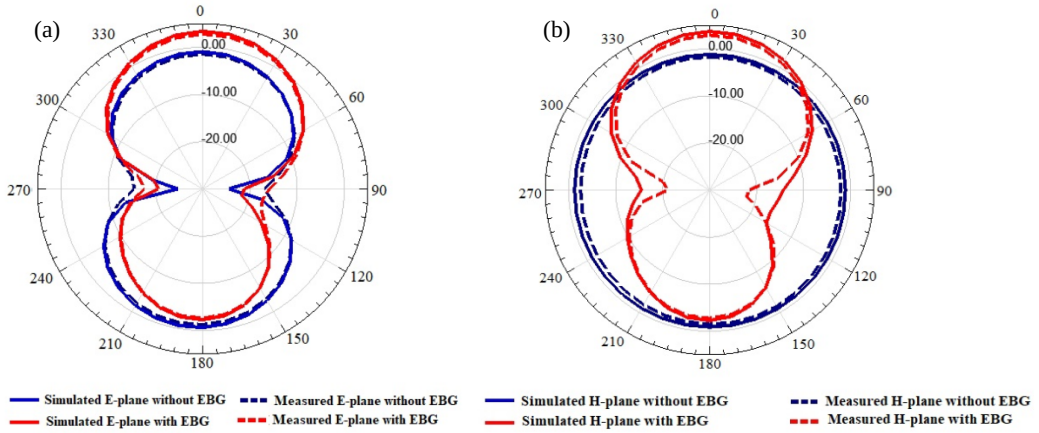

FIGURE 6. Simulated and measured radiation patterns of antenna without EBG and with EBG in (a) E plane and (b) H plane.

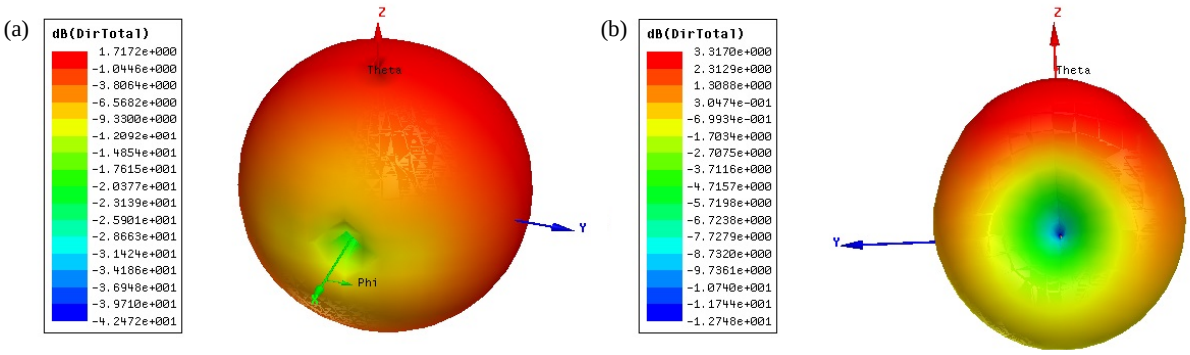

FIGURE 7. Proposed antenna gain. (a) Gain of antenna without EBG. (b) Gain of antenna with EBG.

tor (AMC), thereby suppressing surface-wave propagation and enhancing constructive interference with radiating elements with phase transitioning from -180 to $+180$ degrees away from resonance. The EBG unit cell to get desired reflection phase with geometric parameters is as shown in Figure 4(a) $a = 14$ mm, $b = 7$ mm, $c = 10$ mm, $d = 2$ mm, $e = 1.5$ mm, $f = 9.4$ mm, $g = 14.8$ mm, $h = 8.75$ mm, $i = 3.5$ mm, $j = 2.85$ mm, $k = 7$ mm, $l = 3$ mm, $m =$ mm, $n = 2$ mm. These dimensions helped to get the desired operating frequency by the equations in [20]. The equivalent circuit representation of unit EBG cell is derived in X direction and Y direction as shown in Figures 4(c) and (d). Here, C_1, C_3 are capacitance formed due to slots. C_2, C_4 are the coupling capacitance between patch and substrate. L_1, L_2 are the inductance. EBG unit cell behaves like an LC resonant circuit.

3. ANTENNA EMBEDDED WITH EBG

The designed hexagonal loop shape antenna is put above the EBG array as depicted in Figure 5(a). A 1 mm gap is maintained between the antenna and EBG array to ensure isolation, so no current can flow directly between them (eliminating any direct conductive path or inadvertent shorting), the feed connects only to the antenna patch, not the EBG, ensuring that they stay electrically isolated. Figure 5(b) shows the actual size of fabricated antenna embedded with EBG array. Figure 5(c) shows the measurement setup for antenna characteristics measurements. Figure 5(d) shows the reflection coefficients (simulated and measured) for the antenna with a 2×2 EBG array in free space. In Figure 5(d), the EBG integrated antenna exhibits a simulated resonance at 2.4 GHz with $S_{11} = -32$ dB, while the fabricated prototype resonates at 2.42 GHz with $S_{11} = -27$ dB. The results show a minor shift in the antennas resonant frequency between simulation and measurement, which can come from practical factors such as solder tolerances and SMA connector parasitics. Figure 5(e) shows the comparison of simulated and fabricated S_{11} results of antenna without EBG and with EBG. In Figure 6, E-plane and H-plane radiation patterns of the proposed antenna are compared between simulated and measured results for configurations with and without the EBG, highlighting changes in main beam direction, beamwidth, and sidelobes. Figure 7 shows that the gain of antenna (a) without EBG is 1.7 dB and (b) with EBG is 3.3 dB. The efficiency of an antenna without EBG was about 58%, and after the antenna integration with 2×2 array radiation efficiency increased to 72%.

The proposed antenna with EBG made from jeans fabric as a substrate is tested in three different moisture conditions like dry, water soaked, sweat soaked jeans to understand how moisture affects its return loss and resonance frequency, as shown in Table 1. When the jeans fabric absorbs water or sweat, its dielectric properties change (effective permittivity and loss tangent increase), and return loss degrades due to polar water molecule

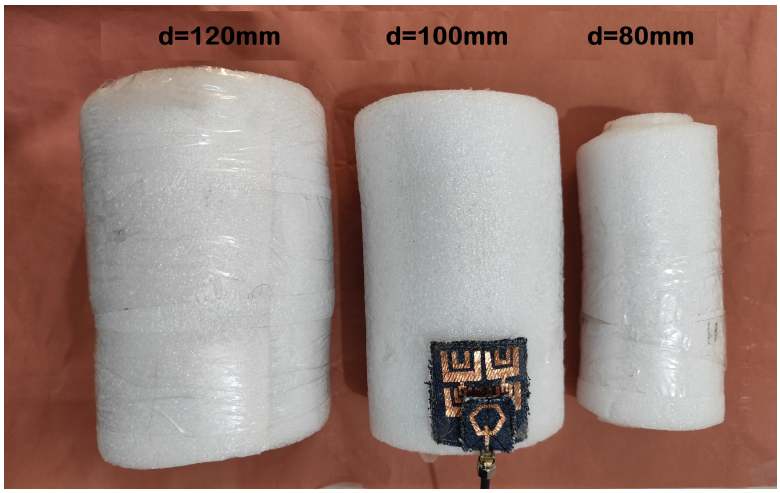

FIGURE 8. Fabricated foam cylinders with varying diameters.

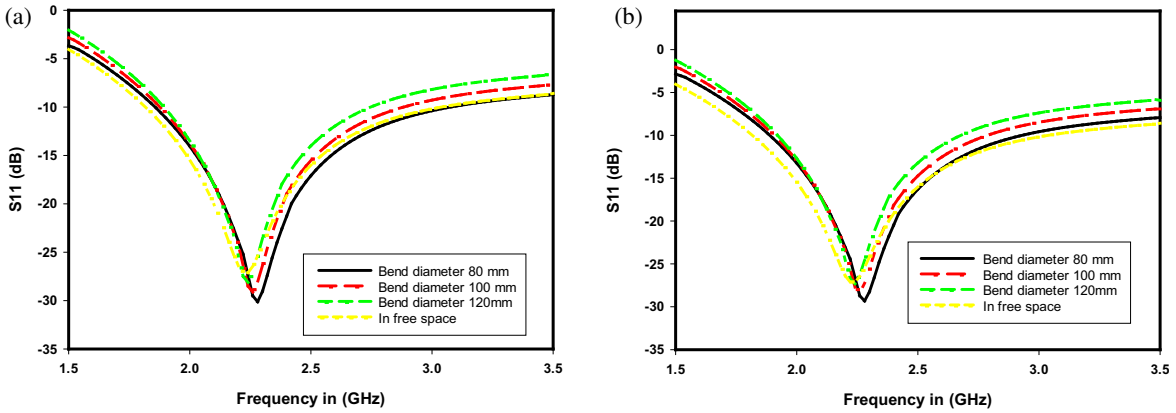

FIGURE 9. S_{11} plots in free space are compared for bending at different diameters in (a) the X direction and (b) the Y direction.

TABLE 1. Antenna performance under moisture.

Moisture state	ε_r	$\tan\delta$	Freq. (GHz)	S_{11} (dB)
Dry	1.78	0.085	2.44	−27.10
Water soaked	3	0.18	2.1	−23.65
Sweat soaked	3.8	0.35	1.72	−17.03

and dissolved ions interact with the electric field of the RF signal [21, 22].

4. BENDING ANALYSIS

To systematically assess the impact of antenna bending when it is placed on body part such as leg and arm, three cylinders with different diameters (120 mm, 100 mm, 80 mm) made from foam were fabricated as shown in Figure 8. These values closely match the diameter of human arm and leg. The proposed antenna is integrated with EBG wrapped on it to study on-body bending. Figure 9 depicts the investigation of measured S_{11} characteristics pertaining to an antenna that is embedded with an EBG structure both in free space and with cylinders exhibiting varying bending diameters in the X and Y orientations [23–24]. It indicates that only small shifts in resonance and bandwidth occur as the bending diameter changes, and these variations are negligible; the antenna maintains its intended operating band and acceptable impedance match.

5. SAR ANALYSIS OF AN EBG-EMBEDDED ANTENNA

For SAR analysis using Ansysy HFSS, a four layer human phantom model comprising skin, fat, muscle, bone characterized by layer specific thickness (T), permittivity (ε_r), conductivity (σ), and density (ρ) as summarized in Table 2 was

TABLE 2. Human tissue parameters at a 2.45 GHz.

Tissue Layer	T (mm)	(ε_r)	σ (S/m)	ρ (Kg/m^3)
Skin	2	37.95	1.491.49	1001
Subcutaneous fat	5	5.27	0.11	900
Muscle	20	52.67	1.77	1006
Cortical bone	13	18.49	0.82	1008

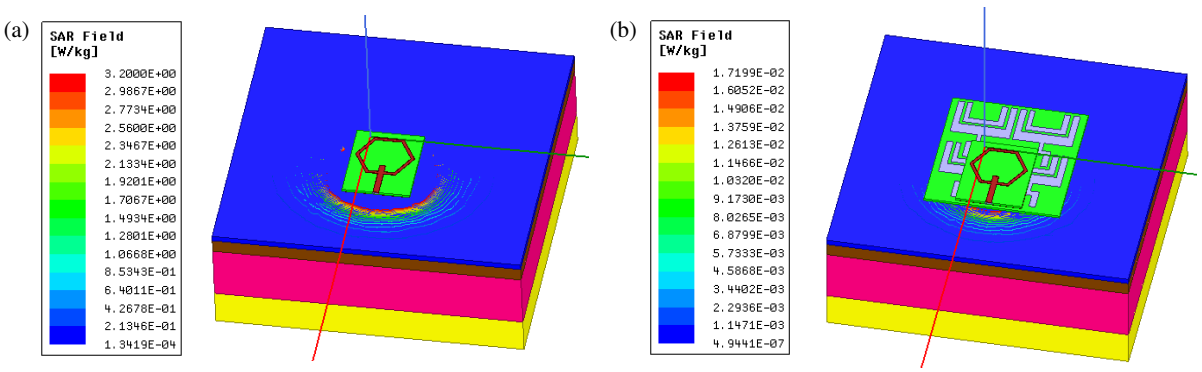

FIGURE 10. Simulated SAR in a four-layer human phantom model: (a) without EBG and (b) with EBG for an input power of 1 W (rms).

TABLE 3. Performance comparison of existing structures with the novel proposed antenna.

Ref.	Size (mm^2)	EBG type & array	Frequen. GHz	SAR in W/kg
13	150×150	Square 3×3	2.45	0.079
14	81×81	Ring shaped pattern 3×3	2.47	0.0554
17	100×100	Square ring 4×4	2.42	0.0464
26	60×60	Square patch with ring slot 2×2	2.45	0.5
27	62×42	Letter I shape 2×2	2.41	0.79
28	68×38	Square patch with square slot 2×1	2.45	0.0244
29	57×57	Dual H shape 3×3	2.45	0.0529
Proposed design	47×43	2×2	2.45	0.0171

FIGURE 11. Antenna placed on human wrist.

used [25]. The input power of 1 W (rms) is used for SAR calculation. The SARs over 1 gm of tissue for two configurations were evaluated first for the proposed antenna alone and then for the antenna embedded with an EBG backing structure designed

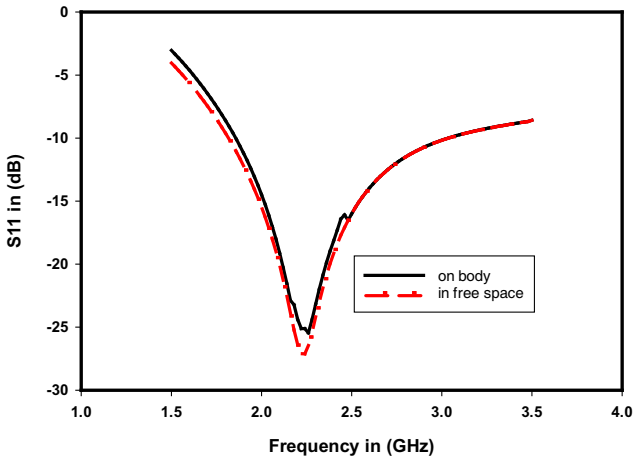

FIGURE 12. S_{11} evaluation of the EBG embedded antenna under free space and on-body placement.

to suppress backward radiation towards the body as shown in Figure 10. For the stand alone antenna, the simulated SAR reached 3 W/kg, indicating substantial near-field coupling into tissues and non-compliance with the 1.6 W/kg FCC specification. For the antenna embedded with EBG, the SAR was reduced to 0.0171 W/kg at 2.45 GHz, demonstrating mitigation and comfortably satisfying the FCC limit. A comparison of the SAR values of antenna alone and antenna with EBG reveals that integrating the EBG structure with antenna leads to significant reduction in SAR, demonstrating its effectiveness in minimizing electromagnetic energy absorption by the body.

For wearable use, it is essential to evaluate antennas flexibility to verify its ability to fit to the human body. Figure 11 presents that the antenna was in a bent state when it was placed on the wrist. To confirm that the designed antenna preserves its resonant frequencies when being placed on human body, its S_{11} was measured in the body worn condition and in free space. The results shown in Figure 12 depict that the resonant frequencies have very close agreement.

A comparative analysis between the proposed antenna embedded with EBG and existing antennae integrated EBG/AMC designs operating at comparable frequency bands is presented in Table 3. It confirms that the proposed antenna embedded with EBG structure carries a compact design and retains SAR level within safety guidelines compared to prior structures

6. CONCLUSION

This research encompasses the design, simulations, fabrication, and critical experimental evaluation of hexagonal loop shape antenna embedded with an EBG structure. The antenna design and EBG structure design are executed utilizing HFSS. The proposed embedded EBG of nested U-shaped rectangular slot with a stretched strip of inverted U shape at bottom as 2×2 array is incorporated with a hexagonal loop shaped patch antenna. This research experimentally validates and endorses that the proposed hexagonal loop shaped patch antenna, incorporated with a novel proposed EBG structure, is appropriate for WBAN applications related to athletic performance evaluation and remote health surveillance. The measured performance of the antenna, with and without the incorporation of EBG structure, exhibits close agreement with the designed values. The measured reflection coefficient S_{11} validates that the antenna integrated with EBG structure succeeds in optimal impedance matching at 2.45 GHz in the ISM band. Along with on-body measurements, a bending analysis wwa performed to examine the antennas mechanical flexibility, and the results demonstrate stable performance under deformation. SAR assessment was executed using a rectangular four layer human tissue model to determine the prototype's viability for body worn application. The inclusion of EBG structures headed to a substantial reduction in SAR, reducing the value from 3 W/kg to 0.0171 W/kg, significantly enhancing the electromagnetic safety of antenna for wearable applications.

REFERENCES

[1] Jalil, M. E. B., M. K. A. Rahim, N. A. B. Samsuri, N. A. Murad, H. A. Majid, K. Kamardin, and M. A. Abdullah, "Fractal koch multiband textile antenna performance with bending, wet conditions and on the human body," *Progress In Electromagnetics Research*, Vol. 140, 633–652, 2013.

[2] Jeong, W., J. Tak, and J. Choi, "A low-profile IR-UWB antenna with ring patch for WBAN applications," *IEEE Antennas and Wireless Propagation Letters*, Vol. 14, 1447–1450, 2015.

[3] Hazarika, B. and B. Basu, "Multi-layered low-profile monopole antenna using metamaterial for wireless body area networks," in *2019 International Conference on Automation, Computational and Technology Management (ICACTM)*, 431–435, London, UK, 2019.

[4] Hu, B., G.-P. Gao, L.-L. He, X.-D. Cong, and J.-N. Zhao, "Bending and on-arm effects on a wearable antenna for 2.45 GHz body area network," *IEEE Antennas and Wireless Propagation Letters*, Vol. 15, 378–381, 2015.

[5] International Commission on Non-Ionizing Radiation Protection (ICNIRP), "ICNIRP guidelines for limiting exposure to time-varying electric, magnetic, and electromagnetic fields (up to 300 GHz)," *Health Physics*, Vol. 74, No. 4, 494–522, 1998.

[6] "IEEE standard for safety levels with respect to human exposure to radio frequency electromagnetic fields, 3 kHz to 300 GHz," in *IEEE Std C95.1-2005 (Revision of IEEE Std C95.1-1991)*, 1–238, 2006.

[7] Guido, K. and A. Kiourti, "Wireless wearables and implants: A dosimetry review," *Bioelectromagnetics*, Vol. 41, No. 1, 3–20, 2020.

[8] El Atrash, M., M. A. Abdalla, and H. M. Elhennawy, "A wearable dual-band low profile high gain low SAR antenna AMC-backed for WBAN applications," *IEEE Transactions on Antennas and Propagation*, Vol. 67, No. 10, 6378–6388, Oct. 2019.

[9] Ashyap, A. Y. I., S. H. B. Dahlan, Z. Z. Abidin, M. I. Abbasi, M. R. Kamarudin, H. A. Majid, M. H. Dahri, M. H. Jamaluddin, and A. Alomainy, "An overview of electromagnetic band-gap integrated wearable antennas," *IEEE Access*, Vol. 8, 7641–7658, 2020.

[10] Abirami, B. S. and E. F. Sundarsingh, "EBG-backed flexible printed Yagi-Uda antenna for on-body communication," *IEEE Transactions on Antennas and Propagation*, Vol. 65, No. 7, 3762–3765, Jul. 2017.

[11] Kim, S., Y.-J. Ren, H. Lee, A. Rida, S. Nikolaou, and M. M. Tentzeris, "Monopole antenna with inkjet-printed EBG array on paper substrate for wearable applications," *IEEE Antennas and Wireless Propagation Letters*, Vol. 11, 663–666, 2012.

[12] Sambandam, P., M. Kanagasabai, S. Ramadoss, R. Natarajan, M. G. N. Alsath, S. Shanmuganathan, M. Sindhadevi, and S. K. Palaniswamy, "Compact monopole antenna backed with fork-slotted EBG for wearable applications," *IEEE Antennas and Wireless Propagation Letters*, Vol. 19, No. 2, 228–232, Feb. 2020.

[13] Velan, S., E. F. Sundarsingh, M. Kanagasabai, A. K. Sarma, C. Raviteja, R. Sivasamy, and J. K. Pakkathillam, "Dual-band EBG integrated monopole antenna deploying fractal geometry for wearable applications," *IEEE Antennas and Wireless Propagation Letters*, Vol. 14, 249–252, 2015.

[14] Gao, G.-P., B. Hu, S.-F. Wang, and C. Yang, "Wearable circular ring slot antenna with EBG structure for wireless body area network," *IEEE Antennas and Wireless Propagation Letters*, Vol. 17, No. 3, 434–437, Mar. 2018.

[15] Ashyap, A. Y. I., Z. Z. Abidin, S. H. Dahlan, H. A. Majid, S. M. Shah, M. R. Kamarudin, and A. Alomainy, "Compact and low-profile textile EBG-based antenna for wearable medical applications," *IEEE Antennas and Wireless Propagation Letters*, Vol. 16, 2550–2553, 2017.

[16] Raad, H. R., A. I. Abbosh, H. M. Al-Rizzo, and D. G. Rucker, "Flexible and compact AMC based antenna for telemedicine applications," *IEEE Transactions on Antennas and Propagation*, Vol. 61, No. 2, 524–531, Feb. 2013.

[17] Yan, S., P. J. Soh, and G. A. E. Vandenbosch, "Low-profile dual-band textile antenna with artificial magnetic conductor plane," *IEEE Transactions on Antennas and Propagation*, Vol. 62, No. 12, 6487–6490, Dec. 2014.

[18] Zhu, S. and R. Langley, "Dual-band wearable textile antenna on an EBG substrate," *IEEE Transactions on Antennas and Propagation*, Vol. 57, No. 4, 926–935, Apr. 2009.

[19] Ahmed, M. I., M. F. Ahmed, and A. H. A. Shaalan, "Novel electro-textile patch antenna on jeans substrate for wearable applications," *Progress In Electromagnetics Research C*, Vol. 83, 255–265, 2018.

[20] Sievenpiper, D., L. Zhang, R. F. J. Broas, N. G. Alexopolous, and E. Yablonovitch, "High-impedance electromagnetic surfaces with a forbidden frequency band," *IEEE Transactions on Microwave Theory and Techniques*, Vol. 47, No. 11, 2059–2074, 1999.

[21] Bonefačić, D. and J. Bartolić, "Embroidered textile antennas: Influence of moisture in communication and sensor applications," *Sensors*, Vol. 21, No. 12, 3988, 2021.

[22] Sandeep, D. R., B. T. P. Madhav, S. Das, N. Hussain, T. Islam, and M. Alathbah, "Performance analysis of skin contact wearable textile antenna in human sweat environment," *IEEE Access*, Vol. 11, 62 039–62 050, 2023.

[23] Keshwani, V. R., P. P. Bhavarthe, and S. S. Rathod, "Eight shape electromagnetic band gap structure for bandwidth improvement of wearable antenna," *Progress In Electromagnetics Research C*, Vol. 116, 37–49, 2021.

[24] Keshwani, V. R., P. P. Bhavarthe, and S. S. Rathod, "Compact embedded dual band EBG structure with low SAR for wearable antenna application," *Progress In Electromagnetics Research M*, Vol. 113, 199–211, 2022.

[25] Stuchly, M. A. and S. S. Stuchly, "Dielectric properties of biological substances — Tabulated," *Journal of Microwave Power*, Vol. 15, No. 1, 19–25, 1980.

[26] Nie, H.-K., X.-W. Xuan, Q. Shi, A. Guo, M.-J. Li, H.-J. Li, and G.-J. Ren, "Wearable antenna sensor based on EBG structure for cervical curvature monitoring," *IEEE Sensors Journal*, Vol. 22, No. 1, 315–323, 2022.

[27] Jiang, Z. H., D. E. Brocker, P. E. Sieber, and D. H. Werner, "A compact, low-profile metasurface-enabled antenna for wearable medical body-area network devices," *IEEE Transactions on Antennas and Propagation*, Vol. 62, No. 8, 4021–4030, Aug. 2014.

[28] Abbasi, M. A. B., S. S. Nikolaou, M. A. Antoniades, M. N. Stevanović, and P. Vryonides, "Compact EBG-backed planar monopole for BAN wearable applications," *IEEE Transactions on Antennas and Propagation*, Vol. 65, No. 2, 453–463, 2017.

[29] Gundre, S. B. and V. R. Ratnaparkhe, "A flexible dual-H shape monopole antenna with dual H shape EBG for WBAN," *Journal of Integrated Science and Technology*, Vol. 13, No. 4, 1072, 2025.